

A Photocatalytic Membrane Reactor for VOC Decomposition Using Pt-Modified Titanium Oxide Porous Membranes

Toshinori Tsuru*, Takehiro Kan-no, Tomohisa Yoshioka and Masashi Asaeda

Department of Chemical Engineering, Hiroshima University

Higashi-Hiroshima, 739-8527 JAPAN

(*corresponding author. E-mail: tsuru@hiroshima-u.ac.jp

Tel: 81-(0)82-424-7714

Fax: 81-(0)82-424-5494)

Abstract

Porous titanium oxide membranes with pore sizes in the range of 2.5 to 22 nm were prepared by a sol-gel procedure, and were applied for decomposition of methanol and ethanol as model volatile organic compounds (VOCs) in a photocatalytic membrane reactor, where oxidation reaction occurs both on the surface and inside the porous TiO₂ membrane while reactants are permeating via one-pass flow. Methanol was completely photo-oxidized by black-light irradiation to CO₂ when methanol at a concentration of 100 ppm was used at a feed flow rate of 500×10^{-6} m³/min, but the conversion decreased when the MeOH concentration in the feed was increased. Pt-modification was carried out by photo-deposition, and led to a decrease in pore diameter. Using Pt-modified membranes, a nearly complete oxidation of methanol up to 10,000 ppm at a feed flow rate of 500×10^{-6} m³/min was observed. Thus, such membranes would be effective for purifying a permeate stream after one-pass permeation through the TiO₂ membranes. The decomposition of ethanol is also discussed.

Keywords: titanium oxide, photocatalysis, catalytic membrane reactor, methanol, platinum, photo-deposition

1. Introduction

Ceramic membranes have attracted a great deal of attention because they have excellent resistance to most organic solvents and can be used over a wide range of temperatures. Titania (titanium oxide, TiO_2), in particular, shows excellent chemical resistance and can be used in both acidic and alkaline solutions, and therefore, titania is one of the most promising materials for the preparation of porous membranes. Titania membranes with pore sizes in the range of nanofiltration (NF) and ultrafiltration (UF) membranes have been successfully prepared by the sol-gel process [1-4]. Moreover, titania, which has three types of crystalline phases, including anatase, rutile, and brookite, shows photocatalytic activities. The principle is based on the generation of photoholes by ultraviolet irradiation and the subsequent generation of OH radicals, caused by reactions with hydroxyl groups adsorbed to the hydrophilic titania surface [5]. Since OH radicals are active for the oxidation of organic compounds, photocatalysis using titania has been extensively investigated for various applications including water and air purification. From the viewpoints of reactor configurations, photocatalytic reactions have conventionally been investigated using TiO_2 powders or coated films on nonporous substrates [6-9]. In such systems, the reactants must diffuse to the TiO_2 surface before photocatalytic reactions can occur. This diffusion process, which is relatively slow, is likely to be a rate-determining step, especially for the case where low concentrations of reactants are fed [9].

We have proposed a photocatalytic membrane reactor in which porous TiO_2 membranes with nanometer sized pores are responsible, not only for selective permeation but also photocatalytic reactions. As schematically shown in Figure 1, oxidation by OH radicals occurs after adsorption either on the surface or inside the porous TiO_2 membrane while reactants are permeating in a one-pass flow. The advantages of the system are (1) the forced transport of reactants by convection to the porous TiO_2 membrane, resulting in an increased reaction rate compared with conventional diffusion transport, and (2) the potential for obtaining a permeate stream oxidized with OH radicals. Photocatalytic membrane reactors have been successfully applied to liquid phase reactions of trichloroethylene [10, 11], where no selective permeation occurred based on the molecular sieving effect, as well as methylene blue [12], the rejection of which was increased by photocatalytic reaction in comparison with that by the molecular sieving effect. Maria et al. [13] also recently demonstrated that a photocatalytic membrane reaction system is effective for enhancing the gas-phase photocatalytic oxidation of trichloroethylene using a nanostructured TiO_2 membrane and a TiO_2 -zeolite hybrid membrane. We reported that the observed reaction rate was increased for the case of photocatalytic membrane reaction than the case of conventional reaction configurations in liquid phase [11] and gas phase reaction [14]. It should be noted that the advantages of a photocatalytic membrane reactor configuration was

mathematically proved by Herz [15].

In this study, porous TiO₂ membranes were prepared by the sol-gel process, and applied to photocatalytic membrane reactions for the gas phase reaction of methanol and ethanol as model volatile organic compounds (VOC). The effect of feed concentration was examined in terms of the conversion of VOCs and the production of intermediates. Moreover, the modification of TiO₂ membranes with platinum was examined in an attempt to increase photocatalytic activity.

2. Experimental

Porous TiO₂ membranes were prepared by the sol-gel process. Titania colloidal sols having various diameters were prepared by the hydrolysis and condensation of titanium tetra-isopropoxide (TTIP) in iso-propanol (IPA) solutions with HCl as a catalyst. TTIP, IPA, H₂O, and HCl were mixed to give a molar ratio of 1: 140: 4: 0.4. The hydrolysis and condensation reactions were carried out for one hour in ice bath, and the sol solutions were then aged at temperatures from 20 to 50 °C for more than 10 hours. Colloidal diameter, which was measured by laser light scattering (ELS8000, Otsuka Electric Co., Japan), could be controlled by the temperature in the aging process. The outer surfaces of cylindrical α -alumina microfiltration membranes (average pore diameter 1 μ m; 1 cm in diameter, 9 cm in length) were coated using anatase particles of 200 nm in diameter (STS-41, kindly supplied by Ishihara Sangyo Kaisha, LTD, Japan) mixed with commercial TiO₂ anatase sol solutions (STS01, kindly supplied by Ishihara Sangyo Kaisha, LTD, Japan) as an intermediate layer. The substrates were coated with colloidal TiO₂ sol solutions and fired at 450 °C, this coating procedure was repeated several times. As shown in Figure 2, the TiO₂ membranes were connected to glass tubing using glass frits; the one end was closed and the other was used to collect the permeate [10-12].

Platinum was photo-deposited on TiO₂ membranes as follows. TiO₂ porous membranes were immersed in chloroplatinic acid aqueous solutions, prepared by dissolving hydrogen hexachloroplatinate hydrate (H₂PtCl₆·6H₂O, Aldrich Chemicals) in ultrapure water, in a Pyrex glass tube. The total weight of the solutions was approximately 19.0 g. After purging the solution with N₂ at an approximate flow rate of 20×10⁻⁶ m³/min for 30 min, the TiO₂ membrane was irradiated by blacklight (BL) for 10-120 min. The initial concentration of chloroplatinic acid was adjusted to 0.6 or 1.9 mol m⁻³. After BL irradiation, the membranes were rinsed by forcing distilled water through the membrane pores, followed by drying at room temperature for 30 min and then at 100 °C for 90min. The Pt concentration in the deposition solutions was determined by ICP analysis, and the amounts of Pt deposited on the TiO₂ membranes were calculated from the concentration change before and after the photo-deposition.

Figure 3 shows a schematic of a photocatalytic membrane reactor; four or eight blacklight (BL) lamps (4 W, main wavelength 350 nm) were mounted approximately at a distance of 60 mm from the center of the quartz membrane cell unit (inner diameter 19 mm, thickness 1 mm) [14]. The light intensity on the surface of the TiO₂ membrane, which was measured by locating optical fibers at the same position as the membrane, was estimated as 4.2 mW/cm² for the case of four BL lamps [14]. Air at a total feed flow rate of 500x10⁻⁶ m³/min was fed from a gas cylinder to the photocatalytic reactor, after a part of the feed flow was bubbled through methanol (MeOH) or ethanol (EtOH) solutions that were maintained at suitable temperatures, so that the feed concentration was controlled in the range of 100 to 13000 ppm (volume-based). Gas compositions were determined by two on-line gas chromatographs using a thermal conductive detector (TCD-GC) within an error of less than 10%. A Porapack T column was used for the analysis of organic components and H₂O, while a Gaskropack54 column was for the analysis of CO₂. The temperature was measured using a thermocouple inserted inside a TiO₂ membrane.

3. Results and Discussion

3.1 Preparation and characterization of TiO₂ membranes

Figure 4 shows an SEM photo of a cross section of a TiO₂ membrane. An intermediate layer with a thickness of several μm was observed on the outer surface of a microfiltration membrane, while the top layer formed by coating colloidal sol solutions was less than 1 μm in thickness. Therefore, the thickness of the TiO₂ layer was approximately several μm including the top layer and the intermediate layer. It should be noted that UV/Vis spectra (Jasco, V-570) of TiO₂ films, which were coated on quartz substrates and fired at 450 °C, revealed that approximately 30 % of BL (350 nm) was estimated to be transmitted through TiO₂ membranes having an approximate thickness of 1 μm. Therefore, it was suggested that BL light penetrated throughout the TiO₂ top layer [12].

The pore size distributions of the TiO₂ membranes were evaluated based on nanoporometry, where a mixture of nitrogen and hexane vapor was fed to the porous membranes and the permeability of nitrogen was measured at different partial pressures of hexane vapor. Hexane vapor is assumed to be capillary-condensed inside membrane pores that are smaller than the Kelvin diameter and block the permeation of nitrogen. A detailed discussion of this principle can be found in our previous papers [16, 17]. The measurements were carried out using a Nanoporometer (Seika Sangyo Co., Tokyo, Japan). Figure 5 shows the dimensionless permeability of nitrogen, normalized with the permeability of dry nitrogen, as a

function of Kelvin diameter. The average pore sizes, defined at 50% of the dimensionless permeability of nitrogen, were controlled in the range of 2 to 17 nm by appropriate choice of the colloidal diameters of the coating solutions [4, 12]. In this study, the permeabilities of nitrogen were in the range of $1-2 \times 10^{-5} \text{ mol s}^{-1} \text{ m}^{-2} \text{ Pa}^{-1}$, which caused the transmembrane pressure drop of 10-20 kPa at the flow rate of $500 \times 10^{-6} \text{ m}^3/\text{min}$. It should be noted that the pore sizes of the intermediate layer were estimated to be several tens of nm, because the spaces among TiO_2 particles having diameters of 200 nm consisted of pores for permeation.

Figure 6 shows an example of the pore size distribution before and after Pt-deposition using 120 min of BL irradiation. The average pore sizes defined at 50 % of the dimensionless permeability of nitrogen, decreased from 16 nm to 10 nm after Pt-modification, suggesting that Pt was deposited on inner or/and outer surface of the TiO_2 through the reduction of chloroplatinic ion by photo-produced electrons, thus reducing the effective pore size. Figure 7 shows the amounts of Pt deposited and the average pore sizes as a function of BL irradiation time. The TiO_2 membranes used in this experiment had average pore sizes of approximately 20 nm before Pt-deposition. With an increase in BL irradiation time, the amount of Pt deposited, which were calculated from the initial concentration and the solution volume, increased and gradually approached a constant value of 2.3 mg, and the average pore sizes by nanoporometry gradually decreased down from 20 nm to 6.9 nm. This tendency appears to be independent of the initial platinum concentration since the amount of Pt deposited appears to be approximately the same at $2 \times 10^{-3} \text{ g}$ for the two initial concentrations of 0.61 and 1.9 mol m^{-3} . This can be explained as follows; once the Pt-layer was formed on the surface of the TiO_2 membranes, BL is not able to penetrate into the TiO_2 layer. Therefore, Pt-deposition ceased and, consequently, the amount of Pt deposited became constant. This effect was explained by Wu et al. [18] who applied this technique to the preparation of hydrogen-selective palladium membranes. The amount of Pt, $2 \times 10^{-3} \text{ g}$ deposited, corresponds to approximately 3 wt% Pt-loading to the TiO_2 , assuming a 9 cm length and a 5 μm thickness for a TiO_2 membrane with a porosity of 40%. At this moment, we have not yet had clear evidence whether the Pt-deposition occurred on the outer surface of TiO_2 membrane or the inner surface of the pores, but it was suggested that the deposition of photo-reduced Pt occurred partly on the inner surface of the TiO_2 pores, since the average pore sizes consistently decreased with BL irradiation time from 20 to 8 nm and approximately 30 % of BL could be transmitted into TiO_2 membranes of 1 μm in thickness.

3.2 Photocatalytic membrane reactor for MeOH decomposition

Figure 8 shows the time course of the concentrations of MeOH, CO₂, HCHO and H₂O at different feed MeOH concentrations, and summarized in terms of conversion and reaction rate in Figure 9. In the run number indicated as ① in Fig. 8, the feed gas bypassed the photocatalytic reactor so as to adjust the MeOH concentration to approximately 100ppm. The photocatalytic reactor was irradiated using eight black-light (BL) lamps, and the radiation heat transfer increased the membrane temperature to approximately 110-120 °C. In run number ②, all the feed gas was permitted to permeate the TiO₂ membrane under BL irradiation. The MeOH concentration in the permeate, that is the concentration at the outlet of the photocatalytic membrane reactor, was reduced to approximately zero ppm. On the other hand, the approximate concentrations of H₂O and CO₂ increased from the feed concentration of 750 ppm and 450 ppm, contained in the compressed air cylinder, to 900 and 550 ppm, respectively. HCHO was not detected in run number ②. This can be explained by forced transport by convection, which is a faster process than diffusion, and better contact between the organic compounds and the TiO₂ surface of the nanosized pores. A photocatalytic membrane reaction, in which all reactants were required to permeate through TiO₂ nanosized pores with a uniform residence time, was reported to show an enhanced reactivity [11, 13-15]. In run numbers ③, ④, and ⑤, the MeOH concentration in the feed was controlled at 1100, 4400, and 2300 ppm, respectively. The methanol and CO₂ concentration in the permeate changed in a stepwise manner and approached a steady concentration for each run. Therefore, it is obvious that the photocatalysis of MeOH is achieved using a thin porous TiO₂ membrane. It should be noted that HCHO, an intermediate product of MeOH oxidation, was not detected in run number ② (low feed concentration), but was detected in run numbers ③, ④, and ⑤ (high feed concentration).

Methanol is oxidized in a consecutive reaction: formaldehyde, formic acid, and then completely oxidized to CO₂. Figure 9 shows the rate of MeOH decomposition, and CO₂ and HCHO production as a function of the feed concentration of MeOH (bottom figure), obtained as the product of air flow rate and the differences in concentration between the feed (C_{feed}) and permeate streams (C_{permeate}), which corresponds to overall reaction rate across the membrane. With an increase in MeOH feed concentration ($C_{\text{MeOH, feed}}$), the rate of decomposition of MeOH increased, reaching a constant value, resulting in a decrease in MeOH conversion (top figure). It should be noted that MeOH conversion was defined as $1 - \frac{C_{\text{MeOH, permeate}}}{C_{\text{MeOH, feed}}}$. This concentration dependency is typically observed for TiO₂ photocatalytic reactions, and has been explained by the Langmuir-Hinshelwood mechanism [6]. The rate of CO₂ production appears to decrease with an increase in feed concentration, and consequently, the conversion of decomposed MeOH to CO₂ (top figure), defined as the ratio of the rate of CO₂ production

divided by the rate of MeOH decomposition, decreased. The rate of production of HCHO increased in a similar manner to MeOH decomposition rate with an increase in MeOH concentration. The suppressed conversion to CO₂ can be attributed to the competitive adsorption of methanol and intermediate products such as formaldehyde. Since the rate of production of HCHO increased in almost the same manner as the decomposition rate of MeOH, the rate limiting process in the complete oxidation does not seem to be the oxidation of methanol to formaldehyde, as was the case of the photo-oxidation of ethanol [19]. The re-adsorption of intermediates and subsequent photo-oxidation, which is essential for complete oxidation, could be restricted by a large amount of methanol in the feed.

The transport mechanism of gases through porous membranes is categorized into the viscous flow, the transition flow, Knudsen flow and the molecular sieving flow with a decrease in the ratio of pore size to the mean free path of gaseous molecules, that is, the Knudsen number (Kn). The transport mechanism of gases through pores in the range of several to several ten nanometers is the Knudsen flow where the mean free path of molecules is greater than the pore diameters and collisions between permeating molecules and pore walls occur more frequently than intermolecular collisions [20]. Therefore, frequent contacts between organic compounds and a TiO₂ surface would be expected to enhance the rate of photocatalytic reaction, and the effect would be pronounced for TiO₂ membranes with smaller pore diameters. Figure 10 shows the effect of pore diameters on the performance of photocatalytic membrane reactors. The decomposition rate of methanol appears to show a tendency to increase with a decrease in the pore diameter of TiO₂ membranes, although MeOH conversion showed a minimum at 6.5 nm probably because of larger feed concentration than the case of 2.5 and 22 nm. Another point which should be addressed is the photocatalytic activities of TiO₂ with nanometer sizes. Crystalline TiO₂ such as anatase and rutile type has been reported to show much higher photocatalytic activity than amorphous TiO₂, because amorphous phase could be sites of recombination of electron-hole pairs. From the viewpoint of pore-size control, amorphous TiO₂ is more appropriate for the preparation of TiO₂ membranes having small pore sizes than crystalline TiO₂ such as anatase and rutile TiO₂ because crystal growth from amorphous to crystalline TiO₂ results in an increase in pore size. Titania membranes in the present study, which were prepared by the sol-gel process, might have low crystallinity with a decrease in pore size, that is, the crystallinity of 2.5 nm membrane might be lower than that of 22 nm membrane. This could be the reason why the conversion of MeOH in Fig. 10 did not increase as greatly as we expected.

The material balance for carbon, based on MeOH, HCHO and CO₂, was approximately 80%, suggesting that other types of intermediates are produced and are possibly adsorbed to

TiO₂ membranes. However, it is obvious that intermediates, including HCHO, a harmful toxic compound, were produced in the photo-oxidation process of MeOH and that the amount of intermediates produced increased with an increase in MeOH feed concentration.

3.3 TiO₂ membranes modified with platinum

The modification of TiO₂ with platinum has been proposed, as a method for increasing the photocatalytic reaction rate. For the case of pure TiO₂, electrons and holes that are created by photo-excitation, recombine inside the TiO₂ or diffuse to the surface and react with molecules adsorbed on the surface. The recombination between electrons and holes decreases the photo-efficiency. It has been proposed that platinum deposits increase the separation of electrons and holes by collecting and trapping electrons. Figure 11 shows photocatalytic decomposition of MeOH using a Pt-modified TiO₂ membrane in which 2.0 mg of Pt was deposited. MeOH, the feed concentration of which was as high as 10000 ppm, was almost completely decomposed, and the conversion to CO₂ was approximately 100%. No HCHO was detected. Thus it is clear that Pt-deposition was quite effective in enhancing photocatalytic activity in comparison with the performance of unmodified TiO₂ membranes as shown in Fig. 9. Therefore, completely purified stream was produced in the permeate stream of TiO₂ membranes.

As discussed in previous papers [19, 21], the addition of a noble metal such as Pt to TiO₂ can cause both photocatalysis as well as thermal catalytic reactions. The radiation heat transfer by the BL lights increased the membrane temperature, which was measured inside the cylindrical membranes, to approximately 110-120 °C. The effect of Pt on the thermal catalytic activity for the decomposition of methanol was investigated by heating the quartz cell by means of a tape-heater. Table 1 summarizes a comparison of methanol decomposition and the conversion of methanol to CO₂. The methanol conversion was 100 % for both photocatalysis (BL on) and thermal decomposition (BL off). On the other hand, the conversion of methanol to CO₂ was 93 % for thermal decomposition, but was increased to 100 % in the case of photocatalysis.

Figure 12 shows a comparison of Pt-modified TiO₂ under black-light (BL) on and off for the decomposition of ethanol as an organic volatile compound. It has been reported that TiO₂ had no thermal reactivity for ethanol oxidation at temperatures up to about 200°C [19], and therefore, the conversion under BL off is due to thermal reactions over the Pt. With an increase in reaction temperature, the ethanol decomposition rate increased more rapidly than the rate of production of CO₂, indicating that thermal catalytic reactions produced more intermediates, such as acetaldehyde, than CO₂ after completion of the oxidation. On the other hand, the conversion of ethanol by photocatalytic reactions were enhanced in comparison with thermal decomposition,

although the conversion of ethanol was small in comparison with that of methanol. Moreover, the decomposed ethanol was more extensively converted to CO₂ by photocatalysis than by the thermal catalytic reaction, suggesting that Pt-modified TiO₂ enhances the complete oxidation of the intermediates produced in the decomposition of ethanol. According to Kennedy and Datye [19], a synergetic effect between photocatalysis and thermal catalytic reactions was reported, that is, the overall conversion of illuminated Pt-modified TiO₂ was larger than the sum of the conversions for photocatalysis and thermal catalytic reactions and the synergetic effect was attributed to the photo-production of acetaldehyde on TiO₂ and its subsequent thermal oxidation over platinum. This effect could be one of the reasons for the enhanced photocatalysis for a photocatalytic membrane reactor.

In conclusion, it is clear that Pt-modification is an effective procedure for increasing the complete oxidation in a photocatalytic membrane reaction system and to produce a purified permeate stream after one-pass reaction.

4. Conclusions

Porous titanium oxide membranes with pore sizes in the range of 2.5 to 22 nm were prepared by the sol-gel process, and were applied to the decomposition of methanol and ethanol as model VOCs in a photocatalytic membrane reactor where oxidation occurs both on the surface and inside the TiO₂ membrane.

1. Methanol was completely photo-oxidized to CO₂ by black-light irradiation in the case of 100 ppm methanol at a feed flow rate of $500 \times 10^{-6} \text{ m}^3/\text{min}$, but the conversion decreased with an increase in MeOH concentration in the feed.
2. With a decrease in pore diameter, the decomposition of methanol shows a tendency to increase probably because of better contact between the TiO₂ pore walls and the permeating reactants.
3. Pt-modification was carried out by photo-deposition, and the average pore sizes decreased with time consistently from 20 to 8 nm. Pt-modified membranes showed an almost complete oxidation up to 10,000 ppm of methanol at a feed flow rate of $500 \times 10^{-6} \text{ m}^3/\text{min}$, and were found to be quite effective for producing a purified permeate stream after a one-pass permeation through porous TiO₂ membranes.
4. The conversion of ethanol by photocatalytic reactions was significantly greater than that by thermal decomposition, and a greater fraction of the decomposed ethanol was converted to CO₂ by photocatalysis than by thermal catalytic reaction. We concluded that Pt-modified TiO₂ enhances the complete oxidation of intermediates produced in the decomposition of

ethanol.

Acknowledgements

This work was supported by Steel Industry Foundation for the Advancement of Environmental Protection Technology and The Salt Science Research Foundation.

REFERENCES

- [1] T. Gestel, C. Vandecasteele, A. Buekenhoudt, C. Dotremont, J. Luyten, R. Leysen, B. Bruggen, G. Maes, Salt retention in nanofiltration with multilayer ceramic TiO₂ membranes, *J. Membr. Sci.*, 209 (2002) 379.
- [2] I. Voigt, G. Fischer, P. Pubhlfürß, M. Schleifenheimer, M. Stahn, TiO₂-NF-membranes on capillary supports, *Sep. Purif. Technol.*, 32 (2003) 87.
- [3] T. Tsuru, Inorganic porous membranes for liquid phase separation, *Separation and Purification Methods*, 30 (2001) 191.
- [4] T. Tsuru, D. Hironaka, T. Yoshioka, M. Asaeda, Titania membranes for liquid phase separation: Effect of surface charge on flux, *Sep. Purif. Technol.*, 25 (2001) 441.
- [5] J. M. Herrmann, Heterogeneous Photocatalysis: Fundamentals and applications to the removal of various types of aqueous pollutants, *Catal. Today*, 53 (1999) 115.
- [6] R. W. Matthews, Photo-oxidation of organic impurities in water using thin films of titanium dioxide, *J. Phys. Chem.*, 91 (1987) 3328.
- [7] M. F. J. Dijkstra, H. Buwalda, A. W. F. de Jong, A. Michorius, J. G. M. Winkelman, A. A. C. M Beenackers, Experimental comparison of three reactor designs for photocatalytic water purification, *Chem. Eng. Sci.*, 56 (2001) 547.
- [8] R. Molinari, M. Mungari, E. Drioli, A. S. Paola, V. Loddo, L. Palmisano and M. Schiavello, Study on a photocatalytic membrane reactor for water purification, *Catal. Today*, 55 (2000) 71.
- [9] C. S. Turchi, D. F. Ollis, Photocatalytic reactor design: an example of mass-transfer limitations with an immobilized catalyst, *J. Phys. Chem.*, 92 (1988) 6853.
- [10] T. Tsuru, T. Toyosada, T. Yoshioka, M. Asaeda, Photocatalytic reactions in a filtration system through porous titanium dioxide membranes *J. Chem. Eng. Japan*, 34 (2001) 844.
- [11] T. Tsuru, T. Toyosada, T. Yoshioka, M. Asaeda, Photocatalytic membrane reactor using titanium oxide membranes, *J. Chem. Eng. Japan*, 36 (2003) 1063.
- [12] T. Tsuru, Y. Ohtani, T. Yoshioka, M. Asaeda, Photocatalytic membrane reaction of methylene blue on nanoporous titania membranes, *Kagaku Kogaku Ronbunshu*, 31 (2005)

108.

- [13] A. J. Maria, W. N. Lau, C. Y. Lee, P. L. Yue, C. K. Chan, K. L. Yeung, Performance of a membrane-catalyst for photocatalytic oxidation of volatile organic compounds, *Chem. Eng. Sci.*, 58 (2003) 959.
- [14] T. Tsuru, T. Kan-no, T. Yoshioka, M. Asaeda, Photocatalytic membrane reactor for gas-phase reaction using porous titanium oxide membranes, *Catal. Today*, 82 (2003) 41-48.
- [15] R. Herz, Intrinsic kinetics of first-order reactions in photocatalytic membranes and layers, *Chem. Eng. J.*, 99 (2004) 237.
- [16] T. Tsuru, T. Hino, T. Yoshioka, M. Asaeda, Permporometry Characterization of microporous ceramic membranes, *J. Membr. Sci.*, 186 (2001) 257.
- [17] T. Tsuru, Y. Takata, H. Kondo, F. Hirano, T. Yoshioka, M. Asaeda, Characterization of sol-gel derived membranes and zeolite membranes by nanoporometry, *Sep. Purif. Technol.*, 32 (2003) 23.
- [18] L.Q. Wu, N. Xu, J. Shi, Novel method for preparing palladium membranes by photocatalytic deposition, *AIChE J.*, 46 (2000) 1075.
- [19] J. C. Kennedy, A. K. Datye, Photothermal heterogeneous oxidation of ethanol over Pt/TiO₂, *J. Catal.*, 179 (1998) 375.
- [20] J. Kärger and D. Ruthven, *Diffusion in Zeolites*, John Wiley & Sons, Inc., 1992, p. 98.
- [21] A. V. Vorontsov, V. P. Dubovitskaya, Selectivity of photocatalytic oxidation of gaseous ethanol over pure and modified TiO₂, *J. Catal.*, 221 (2004) 102.

LIST OF FIGURES

Figure 1 Schematic concept of a photocatalytic membrane reactor.

Figure 2 Schematic view of a tubular TiO₂ membrane.

Figure 3 Schematic diagram of the photocatalytic membrane reactor. (MFM: mass flow meter, BL: black light, GC1: gas chromatograph equipped with a Gaskropack54 column, GC2: gas chromatograph equipped with a Porapak T column, T: thermocouple.)

Figure 4 SEM photo of cross-section of a TiO₂ membrane.

Figure 5 Pore size distribution of TiO₂ membranes, as measured by nanoporometry. (Nanoporometry was carried out for TiO₂ membranes just after membrane preparation, using a mixture of N₂/Hexane at 40 °C.)

Figure 6 Pore size distribution of TiO₂ membranes before and after Pt-modification, as measured by nanoporometry. (Pt-deposited amount was 2 mg after BL irradiation of 120 min. Nanoporometry was carried out using a mixture of N₂/Hexane at 40 °C.)

Figure 7 Average pore sizes and amounts of Pt deposited as a function of black-light irradiation time. (Initial H₂PtCl₆ concentrations: 0.61 and 1.95 mol m⁻³: pore sizes used for this experiment were approximately 20 nm before BL irradiation.)

Figure 8 Time course for the concentration of MeOH, CO₂, HCHO (bottom figure) and H₂O (top figure) in feed and permeate at different feed concentrations. (TiO₂ membrane; MeOH feed concentration =100 ppm for run number ① (bypass) and ②, 1100 ppm for ③, 4400 ppm for ④, and 2300 ppm for ⑤; feed was bypassed in run number ①. Open and closed keys show concentrations in feed and permeate, respectively. In ① and ②, MeOH concentrations multiplied by 10 are shown in the figure.)

Figure 9 Conversion (top figure) and reaction rate (bottom figure) as a function of MeOH concentration in the feed. (TiO₂ membrane; Q_{air}=500x10⁻⁶ m³/min, Membrane temperature=110-120 °C.)

Figure 10 Effect of pore diameter on the performance of photocatalytic membrane reactors. (TiO₂ membrane; MeOH feed concentration: 703 ppm (pore diameters: 2.5 nm), 1050 ppm (6.5 nm), and 667 ppm (23 nm); Q_{air}=500x10⁻⁶ m³/min.)

Figure 11 Conversion (top figure) and reaction rate (bottom figure) as a function of MeOH feed concentration in feed. (Pt-TiO₂ membrane with Pt-deposited amount of 2 mg; Q_{air}=500x10⁻⁶ m³/min.)

Figure 12 Conversion (top figure) and reaction rate (bottom figure) as a function of temperature under black-light on and off. (Pt-TiO₂ membrane with Pt-deposited amount of 0.4mg, EtOH feed concentration: 700 ppm; Q_{air}=500x10⁻⁶ m³/min.)

Table 1 Comparison of photocatalytic performance with and without BL irradiation.

	BL on	BL off
MeOH conversion [%]	100	100
Conversion of decomposed MeOH to CO ₂ [%]	100	93

Pt-modified TiO₂ membrane, Pt-deposited amount=0.4mg.

Feed MeOH concentration 700 ppm, temperature was controlled at 110 °C.

Fig. 1

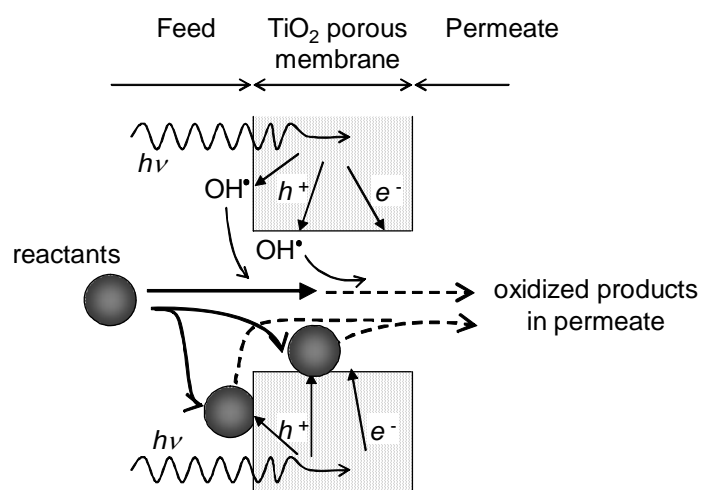


Figure 1 Schematic concept of a photocatalytic membrane reactor.

Fig. 2

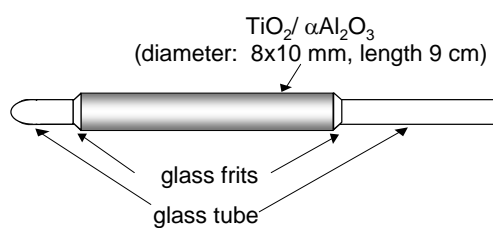


Figure 2 Schematic view of a tubular TiO₂ membrane.

Fig. 3

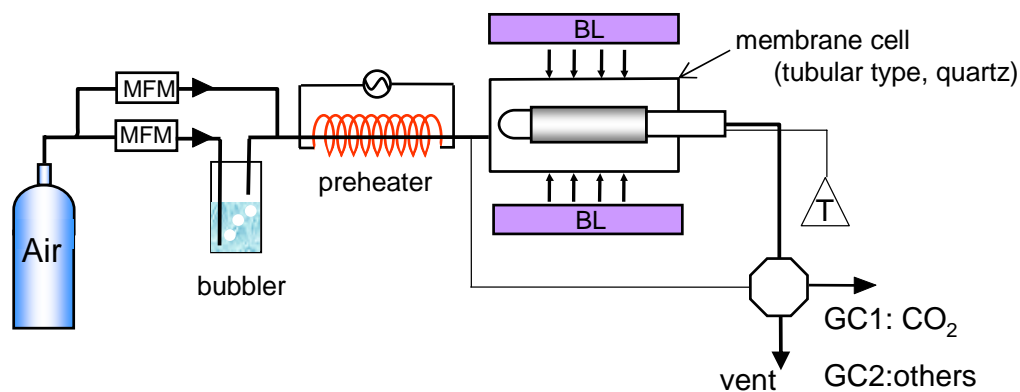


Figure 3 Schematic diagram of the photocatalytic membrane reactor (MFM: mass flow meter, BL: black light, GC1: gas chromatograph equipped with a Gaskropack54 column, GC2: gas chromatograph equipped with a Porapak T column, T: thermocouple.)

Fig. 4

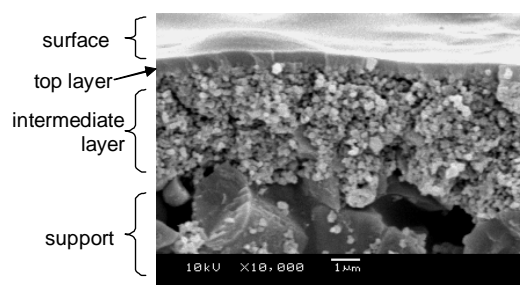


Figure 4 SEM photo of cross-section of a TiO₂ membrane

Fig. 5

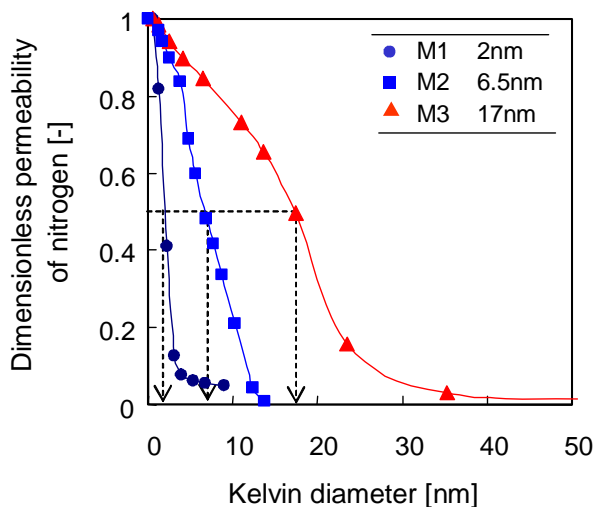


Figure 5 Pore size distribution of TiO₂ membranes, as measured by nanoporometry. (Nanoporometry was carried out for TiO₂ membranes just after membrane preparation, using a mixture of N₂/Hexane at 40 °C.)

Fig. 6

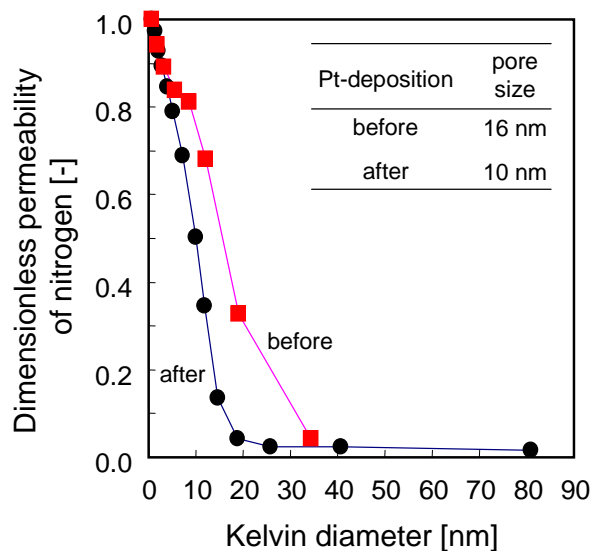


Figure 6 Pore size distribution of TiO₂ membranes before and after Pt-modification, as measured by nanoporometry. (Pt-deposited amount was 2 mg after BL irradiation of 120 min. Nanoporometry was carried out using a mixture of N₂/Hexane at 40 °C)

Fig. 7

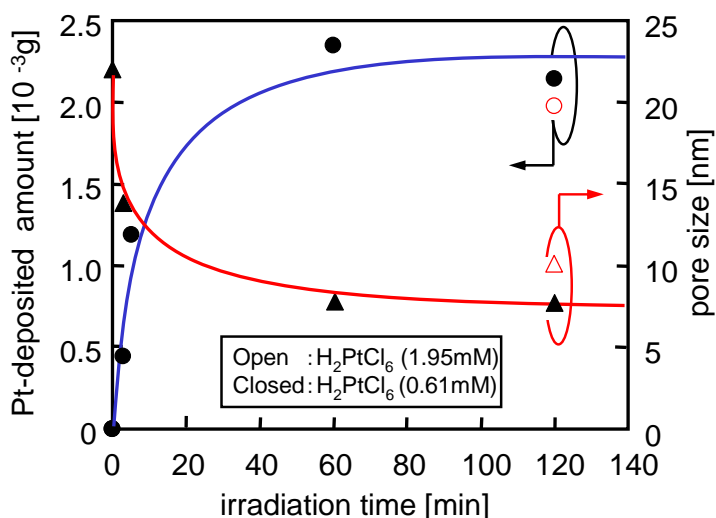


Figure 7 Average pore sizes and amounts of Pt deposited as a function of black-light irradiation time. (Initial H_2PtCl_6 concentrations: 0.61 and 1.95 mol m^{-3} : pore sizes used for this experiment were approximately 20 nm before BL irradiation)

Fig. 8

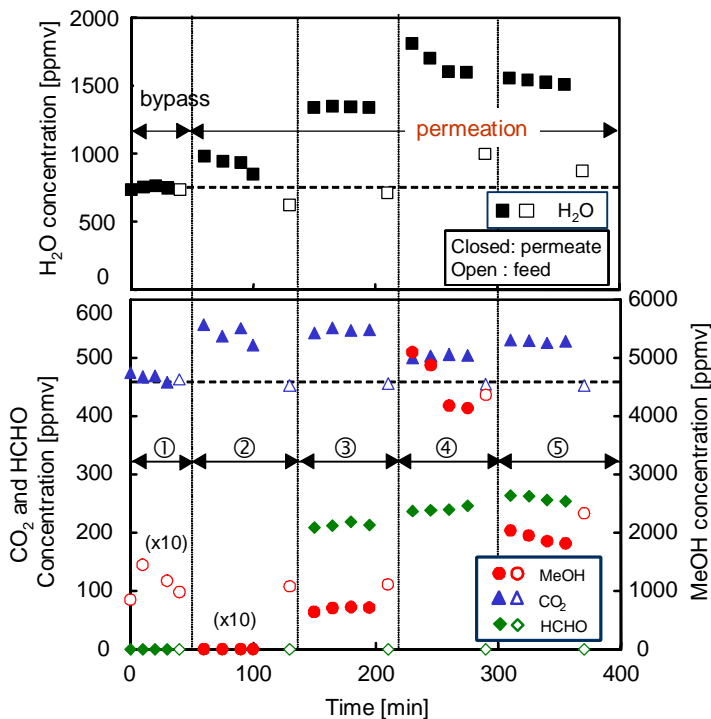


Figure 8 Time course for the concentration of MeOH, CO_2 , HCHO (bottom figure) and H_2O (top figure) in feed and permeate at different feed concentrations. (TiO_2 membrane; MeOH feed concentration = 100 ppm for run number ① (bypass) and ②, 1100 ppm for ③, 4400 ppm for ④, and 2300 ppm for ⑤; feed was bypassed in run number ①. Open and closed keys show concentrations in feed and permeate, respectively. In ① and ②, MeOH concentrations multiplied by 10 are shown in the figure.)

Fig. 9

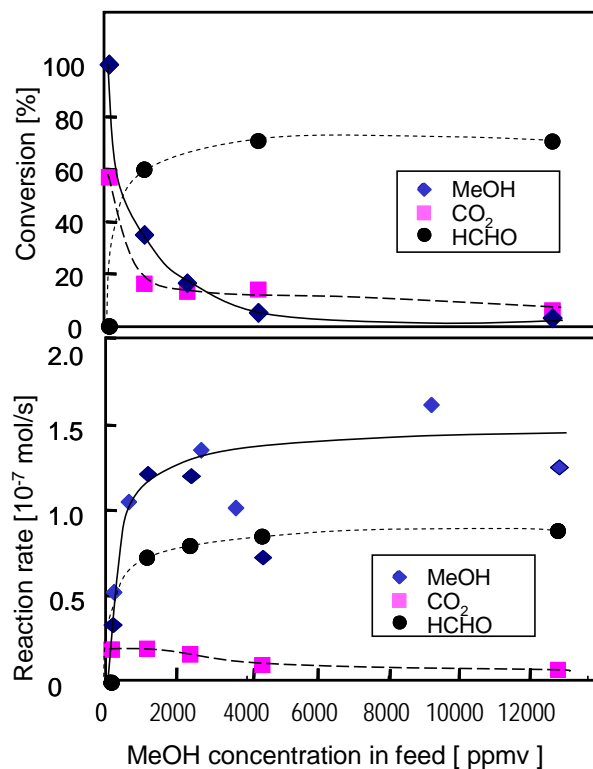


Figure 9 Conversion (top figure) and reaction rate (bottom figure) as a function of MeOH feed concentration in the feed. (TiO₂ membrane; Q_{air}=500x10⁻⁶ m³/min, Membrane temperature=110-120 °C)

Fig. 10

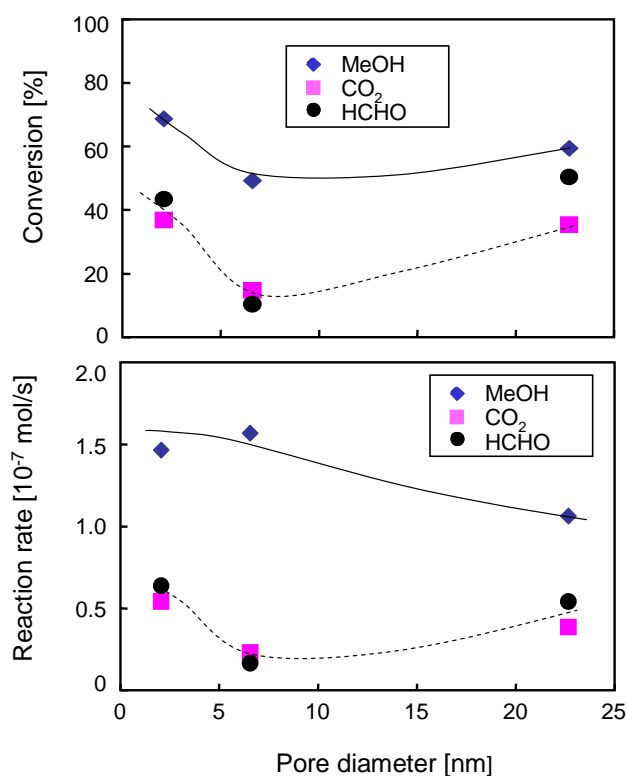


Figure 10 Effect of pore diameter on the performance of photocatalytic membrane reactors (TiO₂ membrane; MeOH feed concentration: 703 ppm (pore diameters: 2.5 nm), 1050 ppm (6.5 nm), and 667 ppm (23 nm); Q_{air}=500x10⁻⁶ m³/min)

Fig. 11

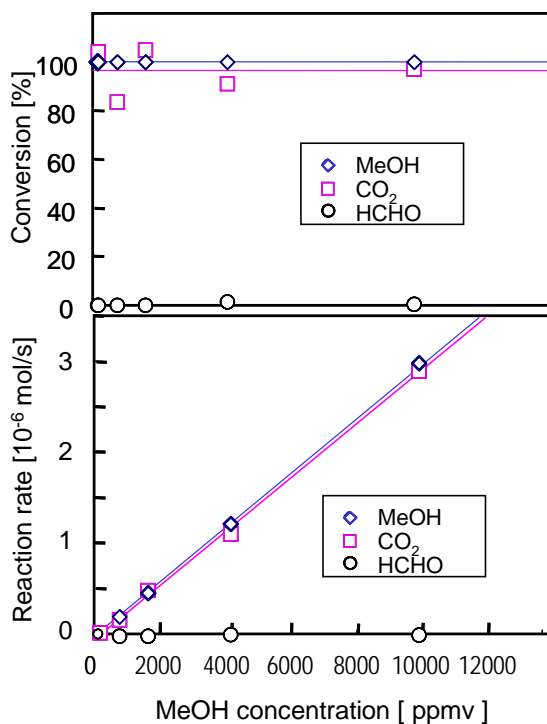


Figure 11 Conversion (top figure) and reaction rate (bottom figure) as a function of MeOH feed concentration in feed. (Pt-TiO₂ membrane with Pt-deposited amount of 2 mg; Q_{air}=500x10⁻⁶ m³/min).

Fig. 12

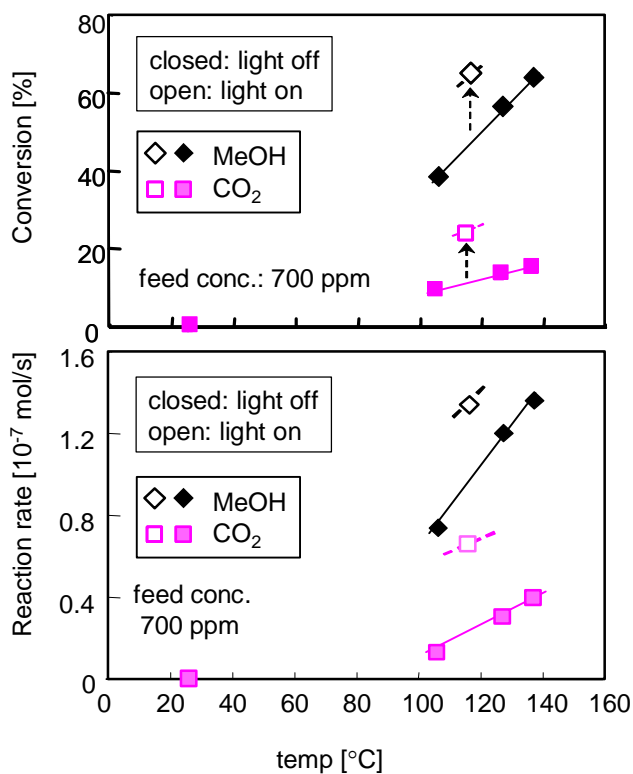


Figure 12 Conversion (top figure) and reaction rate (bottom figure) as a function of temperature under black-light on and off (Pt-TiO₂ membrane with Pt-deposited amount of 0.4mg, EtOH feed concentration: 700 ppm; Q_{air}=500x10⁻⁶ m³/min).